

Controlled quantized adiabatic transport in a superlattice Wannier-Stark ladder

R G Unanyan^{1,*} , N V Vitanov²  and M Fleischhauer¹ 

¹ Fachbereich Physik, University of Kaiserslautern-Landau, Kaiserslautern, D-67663, Germany

² Department of Physics, St Kliment Ohridski University of Sofia, 5 James Bourchier Blvd, 1164 Sofia, Bulgaria

E-mail: unanyan@physik.uni-kl.de

Received 15 August 2022, revised 22 December 2022

Accepted for publication 5 January 2023

Published 2 February 2023



CrossMark

Abstract

The Born–Fock theorem is one of the most fundamental theorems of quantum mechanics and forms the basis for reliable and efficient navigation in the Hilbert space of a quantum system with a time-dependent Hamiltonian by adiabatic evolution. In the absence of level crossings, i.e. without degeneracies, and under adiabatic time evolution all eigenstates of the Hamiltonian keep their energetic order, labeled by a conserved integer quantum number. Thus, controlling the eigenstates of the Hamiltonian and their energetic order in asymptotic limits allows one to engineer a perfect adiabatic transfer between a large number of initial and target states. The fidelity of the state transfer is only limited by adiabaticity and the selection of target states is controlled by the integer invariant labeling the order of eigenstates. We show here, for the example of a finite superlattice Wannier-Stark ladder, i.e. a one-dimensional lattice with alternating hopping amplitudes and constant potential gradient, that such an adiabatic control of eigenstates can be used to induce perfectly quantized single-particle transport across a pre-determined number of lattice sites. We dedicate this paper to the memory of our late friend and colleague Bruce Shore, who was an expert in adiabatic processes and taught us much about this field.

Keywords: adiabatic, Wannier-Stark, quantized transport

(Some figures may appear in colour only in the online journal)

1. Introduction

Quantum adiabatic evolution is a powerful technique rooted in almost century-old ideas. The Born–Fock theorem [1] states that a quantum system remains in an eigenstate of a time-dependent Hamiltonian if there are no level crossings, i.e. no degeneracies, and the change of the parameter of the Hamiltonian is sufficiently slow. Adiabatic evolution can be employed

to transfer a quantum system from one eigenstate of a ‘bare’ Hamiltonian to another one by slowly switching on and off additional coupling terms. Adiabaticity generally requires that the characteristic rate of change of the Hamiltonian is smaller than the interaction energy divided by \hbar . Staying in the same adiabatic state of the full Hamiltonian may then lead to transitions between the bare states, which is usually the objective of the adiabatic approach: to design the Hamiltonian in such a manner that adiabatic evolution can produce a desired transition. Many of the ideas in this field go back to or are strongly influenced by our late friend and colleague Bruce Shore [2]. The great advantage of the adiabatic evolution, and the main reason for its vast popularity, is its insensitivity to variations of the experimental parameters in broad ranges, which sets it apart from the faster but much more

* Author to whom any correspondence should be addressed.



Original Content from this work may be used under the terms of the [Creative Commons Attribution 4.0 licence](https://creativecommons.org/licenses/by/4.0/). Any further distribution of this work must maintain attribution to the author(s) and the title of the work, journal citation and DOI.

fragile resonant techniques. In particular, once the adiabatic condition is satisfied, the transition probability between two quantum states is guaranteed to retain its value despite variations in the experimental conditions.

Over the last century, numerous adiabatic techniques have been designed and demonstrated in a number of groundbreaking experiments, with many contributions from Bruce. Among them we mention adiabatic techniques in two-state systems wherein a major role is played by the presence or absence of an energy level crossing of bare states.

- In the *presence* of a bare-state level crossing the composition of the adiabatic states changes from being aligned with one bare state in the beginning and the other bare state in the end. Therefore, adiabatic evolution produces complete population transfer between the two states. A famous analytic model describing this process is the Landau–Zener–Stückelberg–Majorana model [3–6]. Another beautiful analytic model in this respect is the Allen–Eberly–Hioe model [7, 8]. It is worth mentioning also the half-crossing technique [9, 10], which produces partial, rather than complete population transfer.
- In the *absence* of a bare-state level crossing each adiabatic state is associated with the same bare state in the beginning and the end. Therefore, adiabatic evolution produces no population transfer between the two states. A beautiful analytic model describing this process is the Rosen–Zener model [11]. Despite the absence of population transfer in the no-crossing case, it has valuable applications, e.g. in photon counting in cavity-QED [12, 13].

Quantum systems with more than two states offer a variety of possibilities for navigation in Hilbert space. In particular, level crossing techniques allow to design various navigation pathways. In one approach, the control is achieved by applying the driving pulses at certain level crossings. Hence the evolution is made adiabatic there, while other crossings are left unperturbed and hence the evolution is diabatic in their vicinity. By appropriately combining adiabatic and diabatic evolution one can connect any two states in Hilbert space [14–16]. Such techniques have been used, e.g. for generation of entangled states [17, 18] and molecular superrotors [16]. Alternatively, the frequency chirp of the driving field has been used to transfer the population between the two end states of a chainwise-connected system [19], or from one end of the chain to any pre-selected state [20].

A vastly popular adiabatic technique in multistate systems is stimulated Raman adiabatic passage (STIRAP) [21–23], in which the control of population flow is achieved by using delayed but overlapped driving pulses. STIRAP has been demonstrated and used in hundreds of experiments in dozens of areas, as reviewed recently [24–26]. Although STIRAP has mainly been used for complete population transfer between the two ends of a three-state (original STIRAP) or multistate (extended STIRAP) chainwise-connected systems, variations of this technique for creation of coherent superpositions of states have been successfully demonstrated [27, 28].

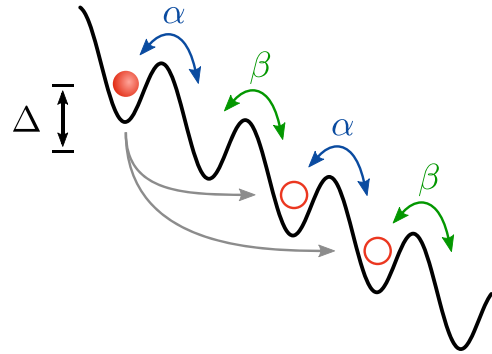


Figure 1. One-dimensional Wannier-Stark ladder in a superpotential with variable and alternating hopping amplitudes α and β and potential gradient Δ . By engineering the asymptotic eigenstates a controlled, quantized particle transport by an arbitrary number of sites and negligible spreading can be achieved.

Finally, the success of adiabatic quantum control techniques over the last decades has triggered the emergence of an entirely new concept in quantum information: adiabatic quantum computation and quantum simulation [29, 30].

An important feature of all adiabatic techniques is that the absence of level crossings guarantees that the integer quantum number characterizing the energetic position of an eigenstate relative to all other states remains the same throughout the adiabatic evolution, while the character of the eigenstate can dramatically change. Thus being able to control the eigenstates of the Hamiltonian only in certain limits (i.e. for the ‘bare’ Hamiltonians), one can induce a perfect state transfer between an initial state and a large number of desired target states by adiabatically changing the parameters of the full Hamiltonian from initial to final values. The selection of target states is entirely controlled by the integer invariant labeling the order of eigenstates and the fidelity of the state transfer is only limited by adiabaticity.

In this paper, we use this concept of adiabatic quantum control to introduce a new technique for quantized adiabatic particle transport. Specifically we consider a quantum particle in a one-dimensional lattice with variable, alternating hopping amplitudes $\alpha(t)$ and $\beta(t)$ subject to a constant potential gradient in the tight-binding limit, see figure 1. Tight-binding lattice Hamiltonians subject to a constant force parallel to the lattice are called Wannier-Stark ladders [31] and their spectral properties and dynamics has extensively been studied in the past. The Wannier-Stark ladder has recently been implemented in arrays of evanescently coupled dielectric waveguides for surface plasmon-polaritons [32].

In the absence of the potential gradient the model of figure 1 is identical to the topological two-band Su–Shrieffer–Heeger model [33]. Adding a time-dependent staggered potential $V(t) = \frac{1}{2} \sum_k (-1)^k \Delta(t)$ leads to the prototype model of a topological particle pump, the Rice-Mele model [34, 35], named after his inventor Thouless pump [36], which was recently implemented in ultra-cold fermions [37], and hard-core bosons [38]. Periodic variation of the parameter of the Rice-Mele Hamiltonian encircling the degeneracy point $\alpha = \beta$ and $\Delta = 0$ leads to a shift of the center of the Wannier functions by exactly

one unit cell. This quantized transport is guaranteed by topology. While the motion of the Wannier center is topologically protected, the wave function of a single particle prepared in a certain lattice site will however quickly spread, such that a Thouless pump is only of limited use in atomtronics for the controlled transport of individual particles [39].

We will show that with the adiabatic pumping technique presented here an arbitrary pre-selected site can be populated, with high selectivity and efficiency, by appropriately tuning the coupling strength between the states. The control concept is rooted in the fact that, as the coupling strength varies, the quantum numbers of the eigenenergies of the respective Hamiltonian change. Hence, when choosing the coupling value in a suitable interval one can navigate adiabatically to the desired final state.

2. Model

We consider a one-dimensional superlattice with N lattice sites in a constant potential gradient as sketched in figure 1. The hopping amplitudes $\alpha(t)$ and $\beta(t)$ are functions of time but with a constant field gradient. In the following we assume an even number $N = M + 1$ for simplicity of the discussion (M being an odd integer). The analysis can however easily be extended to an odd number of sites with essentially similar results, which is discussed in the appendix. In second quantization the Hamiltonian reads

$$H = - \sum_{j,\text{even}} \alpha(t) \hat{c}_{j+1}^\dagger \hat{c}_j - \sum_{j,\text{odd}} \beta(t) \hat{c}_{j+1}^\dagger \hat{c}_j + \text{h.a.} - \sum_{j=-M/2}^{M/2} j \Delta, \quad (1)$$

where \hat{c}_j and \hat{c}_j^\dagger are the particle annihilation and creation operators at lattice site k . In the following we restrict ourselves to the case of a single particle. The Schrödinger equation (we set $\hbar = 1$ throughout this paper) describing the time evolution of the quantum state reads

$$i \frac{\partial}{\partial t} \mathbf{c}(t) = \mathbf{H}_N(t) \mathbf{c}(t), \quad (2)$$

for a system of N Wannier states with probability amplitudes $\mathbf{c}(t) = [c_1(t), \dots, c_N(t)]^T$. The Hamiltonian matrix $\mathbf{H}_N(t)$ has a nondegenerate spectrum and we can order the eigenvalues $\lambda_\mu(t)$ with decreasing value, i.e. $\lambda_1(t) > \lambda_2(t) > \dots > \lambda_N(t)$. The instantaneous eigenvectors of $\mathbf{H}_N(t)$ (called adiabatic states) are denoted by $|\lambda_\mu\rangle$, i.e. $\mathbf{H}_N(t) |\lambda_\mu\rangle = \lambda_\mu |\lambda_\mu\rangle$. In the following, we will assume that the initial state coincides with one of the adiabatic eigenstates of $\mathbf{H}_N(t = -\infty)$.

3. Eight-site Wannier-Stark ladder

Before we consider the general case, let us begin with a system with eight states described by the following Hamiltonian matrix

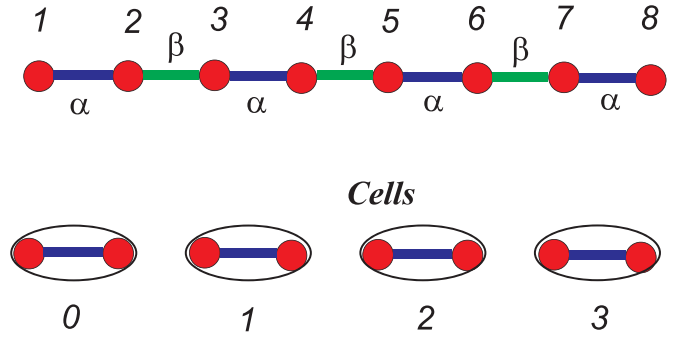


Figure 2. Visualization of linkages and cells of the eight-site Wannier-Stark ladder.

\mathbf{H}_8

$$= \begin{bmatrix} \frac{7}{2}\Delta & \alpha & 0 & 0 & 0 & 0 & 0 & 0 \\ \alpha & \frac{5}{2}\Delta & \beta & 0 & 0 & 0 & 0 & 0 \\ 0 & \beta & \frac{3}{2}\Delta & \alpha & 0 & 0 & 0 & 0 \\ 0 & 0 & \alpha & \frac{1}{2}\Delta & \beta & 0 & 0 & 0 \\ 0 & 0 & 0 & \beta & -\frac{1}{2}\Delta & \alpha & 0 & 0 \\ 0 & 0 & 0 & 0 & \alpha & -\frac{3}{2}\Delta & \beta & 0 \\ 0 & 0 & 0 & 0 & 0 & \beta & -\frac{5}{2}\Delta & \alpha \\ 0 & 0 & 0 & 0 & 0 & 0 & \alpha & -\frac{7}{2}\Delta \end{bmatrix}. \quad (3)$$

$\Delta > 0$ will be used as our unit for frequency. Furthermore we introduce the notation of *cells*, an object containing sites $j = 2k + 1$ and $j = 2k + 2$. In the above model there are four cells: in each unit cell vertices are coupled with each other via hopping amplitude α , and cells are coupled by intercell hopping amplitude β . We use the following numbering scheme for cells (cf figure 2): the cell with site number $j = 2k + 1$ and $j = 2k + 2$ is called k th cell where $k = 0, 1, 2, 3$. In principle, such a model can be implemented in many different physical systems e.g. for neutral cold atoms in an optical superlattice potential [40] subject to an external magnetic field gradient, two-dimensional photonic crystals [41], the two-mode Jaynes–Cummings model [42], or in waveguide structures where time is replaced by the propagation coordinate z [43].

By assuming that the system starts its evolution at the left edge of the chain (the cell with $k = 0$) and the hopping amplitudes are changed slowly (adiabatically) we show that at the end of the (adiabatic) evolution the system ends up at some cell with number k_f . This cell can be pre-selected by an appropriate choice of the asymptotic values of the hopping parameters α and β . The parameter intervals (plateaus) for a fixed k_f are broad enough and are determined by the offset amplitude Δ , such that the transport scheme is robust and does not require fine tuning.

4. Spectral properties of the Hamiltonian

In this section we describe the change of the order of the initial adiabatic energy as function of the hopping amplitudes. First we note that the Hamiltonian (3) is a tridiagonal matrix and therefore all the eigenvalues are non degenerate (simple)

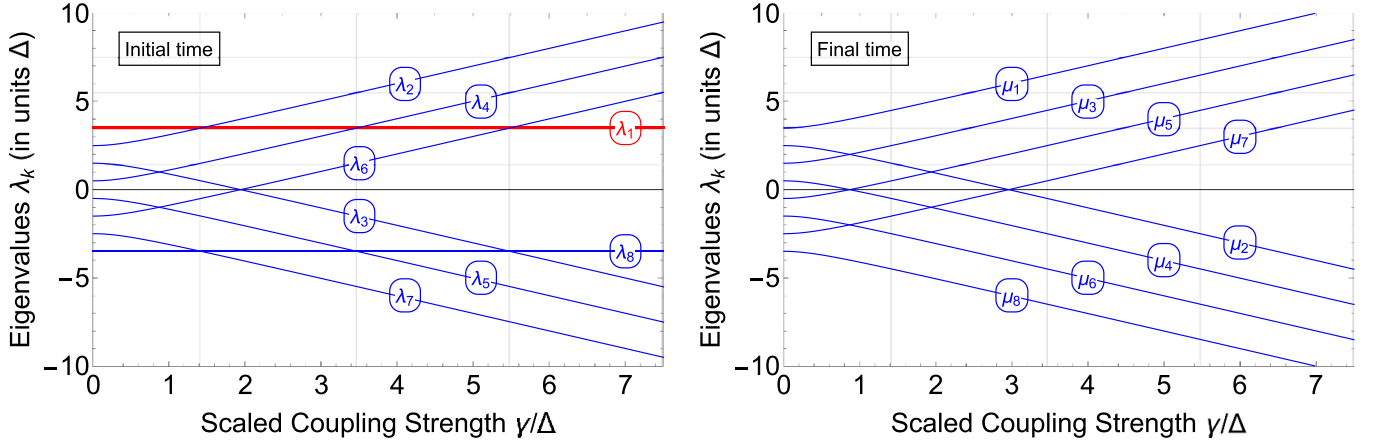


Figure 3. Eigenvalues of the Hamiltonian H_8 (in units Δ) at early and late times vs the scaled coupling strength γ/Δ . Depending on the value of this ratio the initial state $|1\rangle$ can attain any energy-order quantum number in the upper half of the spectrum. Using a negative value of Δ any state in the lower part of the spectrum can be made accessible as well. Note that the degeneracies are accidental since some off diagonals in the Hamiltonian are zero ($\alpha = 0$ for initial time) and ($\beta = 0$, for final time).

if none of the off diagonal matrix elements vanish. The goal of the present paper is to investigate the transport through the cells using slowly changing coupling amplitudes $\alpha(t)$ and $\beta(t)$. We assume that initially ($t \rightarrow -\infty$) the system is in state $|1\rangle$, i.e. in the first cell. Due to the conservation of the order of eigenstates in a time dependent Hamiltonian without true level crossings knowing the spectrum of the Hamiltonian at early and late times determines the transport through cells completely.

To this end we assume that at early times ($t \rightarrow -\infty$) we have $\alpha(-\infty) = 0$ and $\beta(-\infty) = \gamma > 0$. Then the eigenvalues of the Hamiltonian (3) read

$$\begin{aligned} \lambda_1 &= \frac{7}{2}\Delta, & \lambda_2 &= 2\Delta + \frac{1}{2}\sqrt{\Delta^2 + 4\gamma^2}, \\ \lambda_3 &= 2\Delta - \frac{1}{2}\sqrt{\Delta^2 + 4\gamma^2}, & \lambda_4 &= \frac{1}{2}\sqrt{\Delta^2 + 4\gamma^2}, \\ \lambda_5 &= -\frac{1}{2}\sqrt{\Delta^2 + 4\gamma^2}, & \lambda_6 &= -2\Delta + \frac{1}{2}\sqrt{\Delta^2 + 4\gamma^2}, \\ \lambda_7 &= -2\Delta - \frac{1}{2}\sqrt{\Delta^2 + 4\gamma^2}, & \lambda_8 &= -\frac{7}{2}\Delta. \end{aligned} \quad (4)$$

They are plotted in figure 3 (left) versus the scaled coupling strength γ/Δ . The corresponding eigenstates are

$$\begin{aligned} |\lambda_1\rangle &= |1\rangle, \\ |\lambda_2\rangle &= \cos\theta|2\rangle + \sin\theta|3\rangle, & |\lambda_3\rangle &= -\sin\theta|2\rangle + \cos\theta|3\rangle, \\ |\lambda_4\rangle &= \cos\theta|4\rangle + \sin\theta|5\rangle, & |\lambda_5\rangle &= -\sin\theta|4\rangle + \cos\theta|5\rangle, \\ |\lambda_6\rangle &= \cos\theta|6\rangle + \sin\theta|7\rangle, & |\lambda_7\rangle &= -\sin\theta|6\rangle + \cos\theta|7\rangle, \\ |\lambda_8\rangle &= |8\rangle, \end{aligned} \quad (5)$$

where

$$\theta = \frac{\arctan(\gamma/\Delta)}{2}. \quad (6)$$

Because we assume that initially the system is in state $|1\rangle$, this means that in the adiabatic basis, the system begins its evolution in state $|\lambda_1\rangle = |1\rangle$.

For small γ , λ_1 is the maximal eigenvalue of H_8 , with eigenvector $|\lambda_1\rangle = |1\rangle$. However, for γ within $\sqrt{2}\Delta < \gamma < 2\sqrt{3}\Delta$, the eigenvalue λ_1 becomes the second largest. Then, as γ increases beyond $2\sqrt{3}\Delta$, λ_1 becomes the third largest eigenvalue within the interval $2\sqrt{3}\Delta < \gamma < \sqrt{30}\Delta$. Finally when $\sqrt{30}\Delta < \gamma$, λ_1 becomes the fourth largest eigenvalue. Hence, we see that the ‘quantum number’ of the adiabatic state $|\lambda_1\rangle$, i.e. the integer labeling the energetic order, can be varied by changing the coupling value γ . In summary, depending on the choice of the value of γ/Δ , the quantum number n of this adiabatic state $|\lambda_1\rangle$ takes the following integer values:

$$n\left(\frac{\gamma}{\Delta}\right) = \begin{cases} 1 & \text{if } 0 < \frac{\gamma}{\Delta} < \sqrt{2}; \\ 2 & \text{if } \sqrt{2} < \frac{\gamma}{\Delta} < 2\sqrt{3}; \\ 3 & \text{if } 2\sqrt{3} < \frac{\gamma}{\Delta} < \sqrt{30}; \\ 4 & \text{if } \sqrt{30} < \frac{\gamma}{\Delta}. \end{cases} \quad (7)$$

It is remarkable that the sizes of all these intervals are almost equal to 2Δ . Thus one recognizes that choosing the value of γ/Δ allows to preselect a large class of energetic quantum numbers and no fine tuning is needed.

At late times ($t \rightarrow \infty$) we assume that $\alpha(\infty) = \gamma$ and $\beta(\infty) = 0$. Then the eigenvalues of the Hamiltonian (3) are

$$\begin{aligned} \mu_1 &= \frac{6\Delta + \sqrt{\Delta^2 + 4\gamma^2}}{2}, & \mu_2 &= \frac{6\Delta - \sqrt{\Delta^2 + 4\gamma^2}}{2}, \\ \mu_3 &= \frac{2\Delta + \sqrt{\Delta^2 + 4\gamma^2}}{2}, & \mu_4 &= \frac{2\Delta - \sqrt{\Delta^2 + 4\gamma^2}}{2}, \\ \mu_5 &= \frac{-2\Delta + \sqrt{\Delta^2 + 4\gamma^2}}{2}, & \mu_6 &= \frac{-2\Delta - \sqrt{\Delta^2 + 4\gamma^2}}{2}, \\ \mu_7 &= \frac{-6\Delta + \sqrt{\Delta^2 + 4\gamma^2}}{2}, & \mu_8 &= \frac{-6\Delta - \sqrt{\Delta^2 + 4\gamma^2}}{2}. \end{aligned} \quad (8)$$

They are plotted in figure 3 (right) versus the scaled coupling strength γ/Δ . The eigenvalue μ_1 is always the largest. The corresponding eigenstates are:

$$\begin{aligned} |\mu_1\rangle &= \cos\theta|1\rangle + \sin\theta|2\rangle, & |\mu_2\rangle &= -\sin\theta|1\rangle + \cos\theta|2\rangle, \\ |\mu_3\rangle &= \cos\theta|3\rangle + \sin\theta|4\rangle, & |\mu_4\rangle &= -\sin\theta|3\rangle + \cos\theta|4\rangle, \\ |\mu_5\rangle &= \cos\theta|5\rangle + \sin\theta|6\rangle, & |\mu_6\rangle &= -\sin\theta|5\rangle + \cos\theta|6\rangle, \\ |\mu_7\rangle &= \cos\theta|7\rangle + \sin\theta|8\rangle, & |\mu_8\rangle &= -\sin\theta|7\rangle + \cos\theta|8\rangle, \end{aligned} \quad (9)$$

The Born–Fock adiabatic theorem [1] states that if the Hamiltonian varies slowly in time and has well separated eigenvalues at any instant of time then the quantum number of the populated state does not change during evolution. In other words, if the system starts in the eigenstate with the k th largest eigenvalue of the Hamiltonian, it will remain in the eigenstate with the k th largest eigenvalue at all times. We supposed that at $t \rightarrow -\infty$ the initial state was $|1\rangle \equiv |\lambda_1\rangle$ due to the assumption $\alpha(-\infty) = 0$ and $\beta(-\infty) = \gamma > 0$. This adiabatic state has a quantum number $n(\gamma/\Delta)$ depending on the ratio γ/Δ according to equation (7). If we adiabatically change the parameters α and β to values $\alpha(+\infty) = \gamma$ and $\beta(+\infty) = 0$, then the quantum system will remain in the adiabatic state with quantum number $n(\gamma/\Delta)$ for all times. Therefore, we can predict the final state by comparing the left and right frames of figure 3. Because in the beginning of the evolution (left) the system is in the eigenstate $|\lambda_1\rangle$ we have to just count what is the quantum number of this state, i.e. where the eigenvalues

λ_1 is placed. As the ratio γ/Δ increases the quantum number $n(\gamma/\Delta)$ changes from 1 to 4, see equation (7). Adiabatic evolution will therefore transport the population from state $|1\rangle$ to [cf equations (7) and (9), and figure 3]

$$|1\rangle (= |\lambda_1\rangle) \rightarrow \begin{cases} |\mu_1\rangle = \cos\theta|1\rangle + \sin\theta|2\rangle & \text{if } 0 < \frac{\gamma}{\Delta} < \sqrt{2}; \\ |\mu_3\rangle = \cos\theta|3\rangle + \sin\theta|4\rangle & \text{if } \sqrt{2} < \frac{\gamma}{\Delta} < 2\sqrt{3}; \\ |\mu_5\rangle = \cos\theta|5\rangle + \sin\theta|6\rangle & \text{if } 2\sqrt{3} < \frac{\gamma}{\Delta} < \sqrt{30}; \\ |\mu_7\rangle = \cos\theta|7\rangle + \sin\theta|8\rangle & \text{if } \sqrt{30} < \frac{\gamma}{\Delta}. \end{cases} \quad (10)$$

Hence we see that in the adiabatic regime the particle transport is quantized, with the control parameter being the scaled coupling strength γ/Δ . Moreover, in contrast to the Thouless pump, there is no spreading of the particle wave function thereby leading to a perfect single-particle transport.

5. General case

The above results can be easily generalized for an arbitrary odd integer M corresponding to an even number of sites. (We note that the parity of M is however not essential for our protocol and the case of an even M (odd number of sites) is discussed in the appendix.) In this case the Hamiltonian takes the form

$$H_{M+1}(t) = \begin{bmatrix} \frac{M}{2}\Delta & \alpha(t) & 0 & 0 & \dots & 0 & 0 & 0 \\ \alpha(t) & (\frac{M}{2}-1)\Delta & \beta(t) & 0 & \dots & 0 & 0 & 0 \\ 0 & \beta(t) & (\frac{M}{2}-2)\Delta & \alpha(t) & \dots & 0 & 0 & 0 \\ 0 & 0 & \alpha(t) & (\frac{M}{2}-3)\Delta & \ddots & 0 & 0 & 0 \\ \vdots & \vdots & \vdots & \ddots & \ddots & \vdots & \vdots & \vdots \\ 0 & 0 & 0 & 0 & \dots & -(\frac{M}{2}-2)\Delta & \beta(t) & 0 \\ 0 & 0 & 0 & 0 & \dots & \beta(t) & -(\frac{M}{2}-1)\Delta & \alpha(t) \\ 0 & 0 & 0 & 0 & \dots & 0 & \alpha(t) & -\frac{M}{2}\Delta \end{bmatrix}. \quad (11)$$

A simple calculation shows (see appendix) that the quantum number $n(\frac{\gamma}{\Delta})$ does not depend on the dimension of the system size. We have

$$n\left(\frac{\gamma}{\Delta}\right) = \begin{cases} 1 & \text{if } 0 < \frac{\gamma}{\Delta} < \sqrt{2}; \\ 2 & \text{if } \sqrt{2} < \frac{\gamma}{\Delta} < 2\sqrt{3}; \\ 3 & \text{if } 2\sqrt{3} < \frac{\gamma}{\Delta} < \sqrt{30}; \\ 4 & \text{if } \sqrt{30} < \frac{\gamma}{\Delta} < \sqrt{56}; \\ \vdots & \\ k & \text{if } \sqrt{(2k-3)(2k-2)} < \frac{\gamma}{\Delta} < \sqrt{(2k-1)2k} \\ \vdots & \end{cases} \quad (12)$$

With the exception of the first interval, whose length is obviously $\sqrt{2}$, all other intervals have lengths very close to 2,

$$\sqrt{(2k-1)2k} - \sqrt{(2k-3)(2k-2)} = 2 + \frac{1}{4k^2} + O(k^{-3}). \quad (13)$$

Thus controlling the quantum number of the energetic order does not require fine tuning of the parameters. We note that the same analysis can be done when M is an even number (see in the appendix).

6. Numerical results

To illustrate our method we now present numerical results from solving the Schrödinger equation with the Hamiltonian of equation (11). The hopping amplitudes $\alpha(t)$ and $\beta(t)$ are

assumed to be slowly varying functions with the following explicit form

$$\alpha(t) = \frac{\gamma}{\sqrt{1 + \exp(-\frac{t}{\tau})}}, \quad \beta(t) = \frac{\gamma}{\sqrt{1 + \exp(\frac{t}{\tau})}}. \quad (14)$$

The particle is assumed to be in state $|1\rangle$ at $t \rightarrow -\infty$, i.e. in the cell with $k = 0$. In order to describe transport processes on long time scales we calculate the quantity

$$P_\infty = \sum_{k=0}^{\frac{M-1}{2}} k [p_{2k+1}(\infty) + p_{2(k+1)}(\infty)], \quad (15)$$

where k is the number of the cell. The quantity $p_{2k+1}(\infty) + p_{2(k+1)}(\infty)$ is the probability for the particle to be in the k th cell. In fact, P_∞ is equal to the first momentum of the particle distribution. According to the above discussions at the end of the adiabatic evolution the particle will be transmitted through the system in a deterministic quantized fashion. At first glance this process appears much like the Thouless pump [36]. In topological one-dimensional systems the transport is quantized in the adiabatic limit and topologically protected. In the adiabatic limit the displacement of a particle is quantized very precisely in units of the lattice constant. However, as has been shown in [39] in general, the adiabaticity condition give rise also to a large spreading of the wave function in coordinate space. This unavoidable spreading can lead to a smeared-out distribution of particles extending over many unit cells, and from an applicability point of view, this method is rather limited.

We show that our method is capable of removing the unwanted spreading of the particle distribution over cells. Moreover, we show that the variance of the final cell coordinate is bounded from above by a half of the distance between the cells. The variance reaches its maximum at the transition points where the quantum number changes by unity. At these points, the neighbor cells are equally populated and therefore the variance of P_∞ at transition points is equal to

$$\Delta P^2(+\infty) = \frac{k^2 + (k+1)^2}{2} - \left(\frac{k}{2} + \frac{k+1}{2}\right)^2 = \frac{1}{4}. \quad (16)$$

In figure 4 we show the average cell coordinate P_∞ as function of γ for $M = 9, \Delta = 10$. The vertical dashed lines show the borders between different values of the quantum number according to equation (7). The forms of the hopping amplitude are given by equation (14). We see that there is a very good agreement between the results from the numerical analysis and the theoretical prediction of equation (7).

We note that the durations of hoppings $\alpha(t)$ and $\beta(t)$ in equation (14) are unbounded. In order to see the influence of the durations of hopping amplitudes on the transport process we solve the Schrödinger equation (2) with the truncated hopping amplitudes $\alpha(t)$ and $\beta(t)$

$$\alpha(t) = \frac{\gamma}{\sqrt{1 + \exp(-\frac{t}{\tau})}} \Xi\left(\frac{t}{T}\right), \quad \beta(t) = \frac{\gamma}{\sqrt{1 + \exp(\frac{t}{\tau})}} \Xi\left(\frac{t}{T}\right) \quad (17)$$

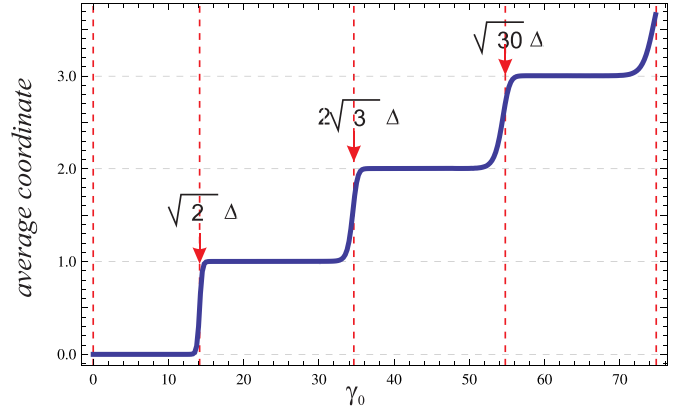


Figure 4. Average final occupation of cells as function of γ for $M = 9, \Delta = 10$ in units of $\tau = 1$. The vertical dashed lines show the border between different values of the quantum number according to equation (7). The form of the hopping amplitudes are given by equation (14).

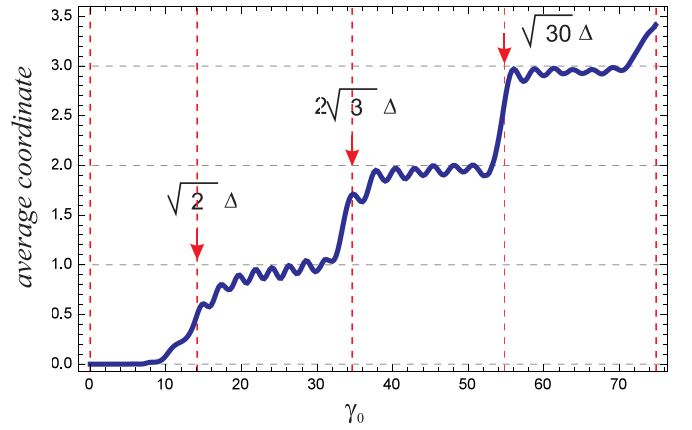


Figure 5. Average final occupation of cells as function of γ for hopping amplitudes given by equation (17) for $T = 7\tau$. The other parameters are the same as in figure 4.

where $\Xi(x)$ represents the unit box function, equal to 1 for $|x| \leq \frac{1}{2}$ and 0 otherwise. As we can see from figure 5 the qualitative behavior of P_∞ remains the same even if the duration T is relative short ($T = 7\tau$).

7. Conclusion

We have proposed an efficient and robust way to navigate the position of a particle adiabatically through a chain of quantum states. The proposed method is similar to the Thouless pumping process, in which the particle displacement, that is the first moment of particle distribution, is quantized. However, in the Thouless pump the second moment (dispersion) of the particle distribution quickly becomes very large. This is because the single particle spreading caused by the finite width of the relevant energy band of the topological lattice model competes with the required adiabaticity of the pump preferring long cycle times. In contrast, we have shown that the state shift in a dynamically modulated Wannier-Stark ladder is also strictly quantized during one adiabatic cycle and at the same time, the

dispersion of the distribution is bounded by one unit cell. The protocol can be implemented, for example, in arrays of evanescently coupled dielectric waveguides [32]. Finally, it should be mentioned that similar ideas can be applied to many-particle systems to study topological phenomena.

Data availability statement

All data that support the findings of this study are included within the article (and any supplementary files).

Acknowledgments

We would like to thank Klaas Bergmann for fruitful and stimulating discussions. R U and M F acknowledge financial support from the Deutsche Forschungsgemeinschaft (DFG) via SFB TR 185, Project No. 277625399. N V V acknowledges support from the European Commission’s Horizon-2020 Flagship on Quantum Technologies Project 820314 (MicroQC).

Appendix

Derivation of equation (12)

In this appendix we elaborate on the derivation of equation (12) of the main text. The Hamiltonian (11) takes a simple block diagonal form in the case when $\alpha = 0$

$$H_{M+1} = \begin{bmatrix} \frac{M}{2}\Delta & 0 & 0 & \dots & \dots & \dots & 0 & 0 & 0 \\ 0 & h_1 & 0 & \dots & \dots & \dots & 0 & 0 & 0 \\ 0 & 0 & h_2 & 0 & \dots & \dots & 0 & 0 & 0 \\ \dots & \dots & \dots & \dots & \dots & \dots & \dots & \dots & \dots \\ \dots & \dots & \dots & \dots & \dots & \dots & \dots & \dots & \dots \\ 0 & 0 & 0 & \dots & \dots & \dots & h_{\frac{M-1}{2}} & 0 & 0 \\ 0 & 0 & 0 & 0 & 0 & 0 & 0 & 0 & -\frac{M}{2}\Delta \end{bmatrix},$$

where each 2×2 matrix h_k has the following form

$$h_k = \begin{bmatrix} (\frac{M}{2} - (2k - 1))\Delta & \gamma \\ \gamma & (\frac{M}{2} - 2k)\Delta \end{bmatrix},$$

$$k = 1, 2, \dots, \frac{M-1}{2}.$$

The spectrum of h_k is

$$\lambda_k^{(+)} = \frac{(M - 4k + 1)\Delta + \sqrt{\Delta^2 + 4\gamma^2}}{2},$$

$$\lambda_k^{(-)} = \frac{(M - 4k + 1)\Delta - \sqrt{\Delta^2 + 4\gamma^2}}{2}.$$

The order of the eigenvalue $\frac{M}{2}\Delta$ can be defined by the following two side condition

$$\lambda_{k-1}^{(+)} \geq \frac{M}{2}\Delta \geq \lambda_k^{(+)}$$

By solving these inequalities with respect to $\frac{\gamma}{\Delta}$, we get

$$\sqrt{2(k-1)(2k-3)} \leq \frac{\gamma}{\Delta} \leq \sqrt{2k(2k-1)} \quad (18)$$

i.e. we arrive at equation (12) of the main text.

Odd number $N = M + 1$ of lattice sites

In the case of an odd number of lattice sites $N = M + 1$ the Hamiltonian takes the following block diagonal form

$$H_{M+1} = \begin{bmatrix} M\Delta & 0 & 0 & \dots & \dots & \dots & 0 & 0 & 0 \\ 0 & h_1 & 0 & \dots & \dots & \dots & 0 & 0 & 0 \\ 0 & 0 & h_2 & 0 & \dots & \dots & 0 & 0 & 0 \\ \dots & \dots & \dots & \dots & \dots & \dots & \dots & \dots & \dots \\ \dots & \dots & \dots & \dots & \dots & \dots & \dots & \dots & \dots \\ 0 & 0 & 0 & \dots & \dots & \dots & h_{M-1} & 0 & 0 \\ 0 & 0 & 0 & 0 & 0 & 0 & 0 & 0 & h_M \end{bmatrix}, \quad (19)$$

where

$$h_k = \begin{bmatrix} (M - (2k - 1))\Delta & \gamma \\ \gamma & (M - 2k)\Delta \end{bmatrix}, \quad k = 1, 2, \dots, M. \quad (20)$$

Repeating the analysis of the main text one obtains the same jump intervals for the quantum numbers $n(\frac{\Delta}{\gamma})$ i.e. (18) or (12). In the case of odd number of sites (M is even number) the step by step quantized adiabatic transport ends however at a ‘lonely’ site, rather than at a pair of sites.

ORCID iDs

R G Unanyan  <https://orcid.org/0000-0001-5926-8093>
 N V Vitanov  <https://orcid.org/0000-0002-8599-4766>
 M Fleischhauer  <https://orcid.org/0000-0003-4059-7289>

References

- [1] Born M and Fock V A 1928 *Z. Phys.* A **51** 165
- [2] Shore B W 1990 *The Theory of Coherent Atomic Excitation* (New York: Wiley)
- [3] Landau L D 1932 *Phys. Z. Sowjetunion* **2** 46
- [4] Zener C 1932 *Proc. R. Soc. A* **137** 696
- [5] Stückelberg E C G 1932 *Helv. Phys. Acta* **5** 369
- [6] Majorana E 1932 *Nuovo Cimento* **9** 43
- [7] Allen L and Eberly J H 1975 *Optical Resonance and Two-Level Atoms* (New York: Dover)
- [8] Hioe F T 1984 *Phys. Rev. A* **30** 2100
- [9] Yatsenko L P, Vitanov N V, Shore B W, Ricketts T and Bergmann K 2002 *Opt. Commun.* **204** 413
- [10] Zlatanov K N and Vitanov N V 2017 *Phys. Rev. A* **96** 013415
- [11] Rosen N and Zener C 1932 *Phys. Rev.* **40** 502
- [12] Raimond J M, Brune M and Haroche S 2001 *Rev. Mod. Phys.* **73** 565
- [13] Nogues G, Rauschenbeutel A, Osnaghi S, Brune M, Raimond J M and Haroche S 1999 *Nature* **400** 239
- [14] Rangelov A A et al 2005 *Phys. Rev. A* **72** 053403
- [15] Oberst M, Münch H and Halfmann T 2007 *Phys. Rev. Lett.* **99** 173001
- [16] Vitanov N V and Girard B 2004 *Phys. Rev. A* **69** 033409
- [17] Unanyan R G, Vitanov N V and Bergmann K 2001 *Phys. Rev. Lett.* **87** 137902
- [18] Unanyan R G, Fleischhauer M, Vitanov N V and Bergmann K 2002 *Phys. Rev. A* **66** 042101
- [19] Broers B, van Linden van den Heuvell H B and Noordam L D 1992 *Phys. Rev. Lett.* **69** 2062

- [20] Melinger J S, Gandhi S R, Hariharan A, Goswami D and Warren W S 1994 *J. Chem. Phys.* **101** 6439
- [21] Vitanov N V, Fleischhauer M, Shore B W and Bergmann K 2001 *Adv. At. Mol. Opt. Phys.* **46** 55
- [22] Gaubatz U, Rudecki P, Schieman S and Bergmann K 1990 *J. Chem. Phys.* **92** 5363
- [23] Bergmann K, Theuer H and Shore B W 1998 *Rev. Mod. Phys.* **70** 1003
- [24] Bergmann K *et al* 2019 *J. Phys. B: At. Mol. Opt. Phys.* **52** 202001
- [25] Vitanov N V, Rangelov A A, Shore B W and Bergmann K 2017 *Rev. Mod. Phys.* **89** 015006
- [26] Bergmann K, Vitanov N V and Shore B W 2015 *J. Chem. Phys.* **142** 170901
- [27] Unanyan R G, Shore B W and Bergmann K 1999 *Phys. Rev. A* **59** 2910
- [28] Theuer H, Unanyan R, Habscheid C, Klein K and Bergmann K 1999 *Opt. Express* **4** 77
- [29] Farhi E, Goldstone J, Gutmann S and Sipser M arXiv:quant-ph/0001106
- [30] Das A and Chakrabarti B K 2008 *Rev. Mod. Phys.* **80** 1061
- [31] Glück M, Kolovsky A R and Korsch H J 2002 *Phys. Rep.* **366** 103
- [32] Wetter H, Fedorova Z and Linden S 2022 *Opt. Lett.* **47** 15
- [33] Su W P, Schrieffer J R and Heeger A J 1979 *Phys. Rev. Lett.* **42** 1698
- [34] Rice M J and Mele E J 1982 *Phys. Rev. Lett.* **49** 1455
- [35] Asboth J K *et al* 2016 *A Short Course on Topological Insulator: Band Structure and Edge States in One and Two Dimensions (Lecture Notes in Physics vol 919)* (Berlin: Springer)
- [36] Thouless D J 1983 *Phys. Rev. B* **27** 6083
- [37] Nakajima I S, Tomita T, Taie S, Ichinose T, Ozawa H, Wang L, Troyer M and Takahashi Y 2016 *Nat. Phys.* **12** 296
- [38] Lohse M, Schweizer C, Zilberberg O, Aidelsburger M and Bloch I 2016 *Nat. Phys.* **12** 351
- [39] Wawer L, Unanyan R and Fleischhauer M arxiv:2110.12280
- [40] Bloch I, Dalibard J and Zwirger W 2008 *Rev. Mod. Phys.* **80** 885
- [41] Ozawa T *et al* 2019 *Rev. Mod. Phys.* **91** 015006
- [42] Jaynes E T and Cummings F M 1963 *Proc. IEEE* **51** 89
- [43] Shore B W and Knight P L 1993 *J. Mod. Opt.* **40** 1195
- Unanyan R G and Fleischhauer M 2002 *Phys. Rev. A* **66** 032109
- [43] Fedorova Z, Jörg C, Dauer C, Letscher F, Fleischhauer M, Eggert S, Linden S and von Freymann G 2019 *Light: Sci. Appl.* **8** 63